Delineating the Role of Transporters in the Absorption and Disposition of Digoxin Using the Physiologically Based Pharmacokinetic (PBPK) Modeling

T0930-02-11

Suvarchala Avvari, Revathi Chapa, Jeffry Adiwidjaja, Rebecca Graves, Viera Lukacova

Simulations Plus, Inc., Lancaster, California, USA

CONTACT INFORMATION: suvarchala.avvari@simulations-plus.com

PURPOSE

Digoxin (DIG) is one of the cardiac glycosides that inhibits sodium-potassium ATPase, an enzyme that regulates the intracellular concentration of sodium and potassium. DIG falls under Class IV of the Biopharmaceutics Classification System (BCS), i.e., a low solubility and low permeability and is the most commonly recommended probe substrate to investigate the drug-drug interaction (DDI) potential of investigational drugs that are P-gp inhibitors and/or inducers. The absorption and disposition of DIG is governed by multiple transporters: P-gp, MDR3, OATP4C1, and Na^+/K^+-ATPase.

OBJECTIVE(S)

The purpose of this project was to 1) develop a mechanistic PBPK model delineating the role of transporters in the absorption and disposition of DIG, and 2) verify the contributions of transporters by simulating clinical DDIs studies with rifampicin (RIF), itraconazole (ITZ), and clarithromycin (CLM).

METHOD(S)

The GastroPlus® v.9.8.3 was used to build and validate DIG PBPK model. The Advanced Compartmental Absorption and Transit (ACAT™) model was used to describe the intestinal dissolution and absorption of DIG after PO administration, and PBPKPlus™ module was used to describe DIG systemic distribution and elimination. Human physiologies were generated using the Population Estimates for Age-Related Physiology (PEAR Physiology™) module within the GastroPlus. The systemic distribution of DIG was described using a whole body PBPK model with a permeability-limited model for kidney and muscle and a perfusion-limited model for the remaining tissues. Tissue/plasma partition coefficients were calculated from tissue composition and compound physiochemical properties using the default methods (Lukacova for perfusion-limited and Poulin and Theil -extracellular for permeability-limited tissues). The passive diffusion permeability-surface area products or PStc for tissues described by a permeability-limited model were calculated from Specific PStc (Spec.PStc) value that is fitted to the IV data[4,13,14] (PStc per mL of tissue cell volume) and the individual tissue cell volumes. The impact of the OATP4C1-mediated influx at the basolateral side and P-gp efflux at the apical side of kidney proximal tubules on DIG renal secretion and the basolateral uptake of DIG into muscle tissue through Na^+/K^+-ATPase[1,2,3] was included in the model (Figure 1). DIG biliary secretion was modeled by simple flux across the apical liver membrane by fitting the PStc of 0.5 mL/s such that the biliary secretion represents ~25% of the total drug elimination. The key physicochemical and biopharmaceutical parameters used to build the DIG model are listed in Table 1. The DDI module in GastroPlus was used to predict the effect of RIF, ITZ, and CLM on DIG PK for varying study designs[4-12]. Table 2 summarizes the induction and inhibition parameters for perpetrator drugs used in the DDI simulations.

Figure 1: Transport, Metabolism, and Elimination Pathways of Digoxin

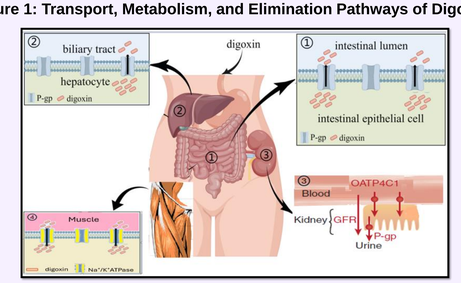

RESULT(S)

Figure 2 presents the Cp-time profiles following Single IV doses ranging from 0.5 mg to 1.5 mg and a single PO dose of 1mg. Figure 3 presents the Cmax and AUC predictions for clinical studies used for DIG model development and validation. The model accurately captures the DIG PK after single dose IV and PO administrations of doses ranging from 0.25 mg to 1 mg in fasted or fed state, with more than 70% of the predicted Cmax and AUC values within the bioequivalence (BE) limit of 0.8-1.25, 95% of predictions within 50% of the observed data, and all the predictions were within 2-fold of the observed data [5-20]. DIG C_p-time profiles before and during co-administration with interacting drugs were reasonably predicted over the full range of administered doses. The predicted Cmax and AUC ratios were mostly within the Guest limits[21] as shown in Figure 4. It is worthwhile to notice the RIF impact, which depending on the timing of DIG and RIF administration, may show a net induction effect (ratio < 1) or net inhibition effect (ratio > 1), and the model accurately captured these scenarios (orange points in Figure 4).

Table 1: Key Physicochemical and Biopharmaceutical Parameters for Digoxin Used in GastroPlus Simulations

Parameter	Value
Molecular weight	780.96 [22]
logP	1.26 [22]
Diffusion coefficient[a]	0.44x10^{-5} cm^2/s
pKa	NA
Reference solubility	0.058 mg/mL @ pH = 7.0 [23]
Dissolution Model	Johnson with a Particle size of 5 um [24]
Precipitate radius	1 µm
Drug particle density	1.2 g/mL
Mean precipitation time	900 s
Human Jejunal P_{eff} (×10^{-4})[b]	1.765 cm/sec
Blood: plasma concentration ratio (R_{BP})	0.55 [Fitted]
Percent unbound in plasma (F_{up}%)	75 [26]
Adjusted percent unbound in plasma (%)[c]	69.249
OATP4C1 **(kidney, basolateral influx)**	
K_m (µM)	7.8 [1]
V_{max} (mg/s/mg trans protein)	0.1 [Optimized]
Na^+/K^+-ATPase **(muscle, basolateral influx)**	
K_m (mg/L)	6.2 [Assumed]
V_{max} (mg/s/mg trans protein)	0.03 [Optimized]
P-gp **(liver and kidney apical efflux, brain basolateral efflux)**	
K_m (µM)	177 [2]
V_{max} (mg/s/mg trans protein)	0.018 [Optimized]
P-gp **(gut-apical efflux)**	
K_m (µM)	177 [2]
V_{max} (mg/s/mg trans protein)	0.15 [Optimized]
Liver Apical PStc	0.5 (mL/s) [Fitted]
SpecPStc	0.35 (mL/s/mL) [Optimized]

[a] Predicted using ADMET Predictor v9.5 (Simulations Plus 2019)
[b]GastroPlus built-in Rat P_{eff}-to-P_{eff} conversion using experimental rat permeability 0.4 ×10^{-4} cm/s [25]
[c] Adjusted F_{up} was calculated from experimental F_{up} and logD @ pH = 7.4 using the default GastroPlus equation (SimulationsPlus 2021).

Table 2 Induction and Inhibition parameters for Rifampicin, Itraconazole, and Clarithromycin used in DDI predictions

Parameter	Value
Itraconazole	
P-gp IC_{50},in vitro, u	0.2 µM [27]
CYP3A4 Ki, in vitro, u	1.3 µM [28]
OH- ITZ CYP3A4 Ki, in vitro, u	295 µM [28]
Keto- ITZ CYP3A4 Ki, in vitro, u	4 µM [28]
ND- ITZ CYP3A4 Ki, in vitro, u	110 µM [28]
Clarithromycin	
P-gp Ki, in vitro, u	4.1 µM [29]
Rifampicin	
***CYP3A4**	
EC_{50}, in vitro, u	0.064 µM [30]
Emax	15 [Fitted]
Ki, in vitro, u	18.5 µM [31]
***UGT1A3**	
EC_{50}, in vitro, u	0.064 µM [30]
Emax	4.4 [Fitted]
***MRP2 Ki, in vitro, u**	0.87 µM [32]
***OATP1B1 Ki, in vitro, u**	0.07 µM [33]
P-gp	
EC_{50}, in vitro, u	0.064 µM [34]
Emax	2.2 [35]
IC_{50}, invitro, u	0.49 µM [34]

Note : *CYP3A4, UGT1A3, MRP2, and OATP1B1 impact PK of rifampicin and its metabolite, CYP3A4 impact PK of itraconazole and its metabolites and were included in the model to ensure accurate RIF and ITZ PK prediction

Figure 2 : PBPK Model development of Digoxin

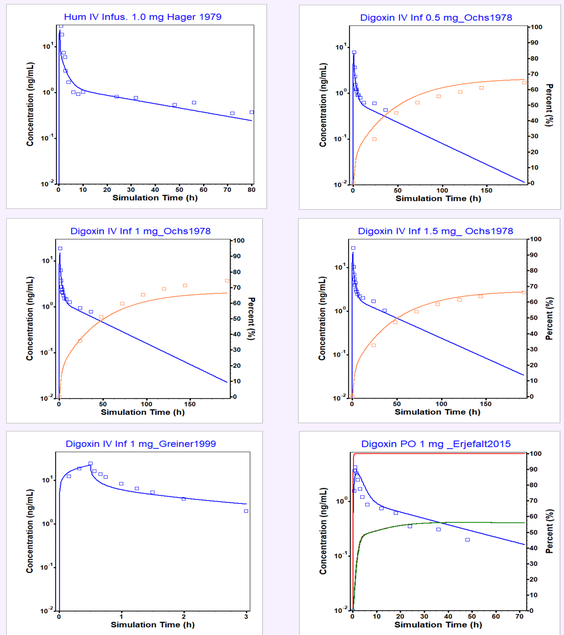

Cp-time profile for a IV infusion dose ranging from 0.5 mg to 1.5 mg and 1 mg oral solution dose of Digoxin in Healthy subjects.
Observed blue squares, simulated blue line of digoxin (Hager et al. 1979, Ochs et al. 1978, Greiner et al. 1999, Erjefalt et al. 2015). The plot also displays observed orange squares, and simulated orange line of percent excreted in urine, simulated total amount of dose dissolved (red), absorbed (brown), entered portal vein (green) as a percent of total administered IV infusion and oral dose of digoxin.

Figure 3: Predicted versus observed DIG PK parameters (a) C_{max} (b) AUC_{0_t}

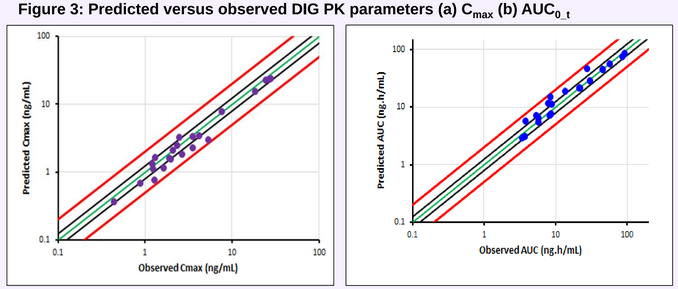

Goodness-of-Fit Plots Showing the Predicted vs Observed Values for C_{max} and AUC_{0_t} of Digoxin of All Studies

Purple circles and Blue Circles represent the predicted vs observed values for C_{max} and AUC of digoxin and the red lines (——) represent 2-fold prediction error, Black lines (——) represent the 1.25-fold prediction error.

Figure 4 Observed vs Predicted Cmax and AUC Ratio for DDI Between DIG and P-gp inducer and inhibitors RIF, ITZ and CLM

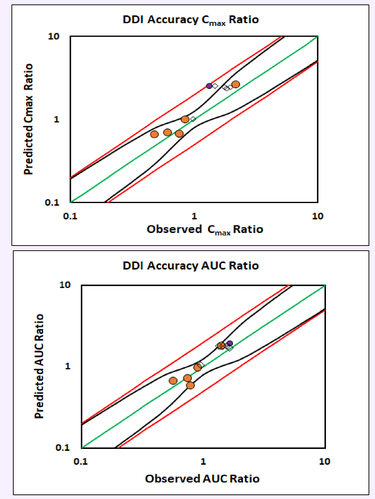

Fig 4 illustrates the DDI Cmax AUC ratios of Digoxin- RIF, ITZ, and CLM DDIs. The green, red, and black lines indicate the line of identity, 2-fold acceptance limits, and acceptance limits suggested by Guest et. al (Guest EJ. et al., DMD. (2011) 39 :170)

CONCLUSION(S)

The work here aimed to develop the DIG PBPK model and validate it as a sensitive substrate model for use in predicting the potential DDI interactions between DIG and P-gp perpetrators. The PBPK approach incorporates all the relevant processes in drug ADME, and all the perpetrator mechanisms. The overall results presented in Figures 2,3, and 4 show that the model accurately captures DIG PK and predicts the effect of perpetrators on IV and PO doses of DIG. The validated DIG model can be used to evaluate potential DDI interactions with other P-gp perpetrators.

REFERENCES

1. Mikkaichi. Proc Natl Acad Sci USA., 101(10):3569 (2004)
2. Troutman. Pharm Res., 20(8):1200 (2003)
3. Lee CA. CPT., 96(3):298 (2000)
4. Greiner. J Clin Invest., 52(7):147 (1999)
5. Wiebe. Clin Pharmacokinet., 59:1627 (2020)
6. Kirby. Drug Metab Dispos.,40(3):610 (2012)
7. Gurley. Mol Nutr Food Res., 52(7):772 (2008)
8. Jalava. Therap Drug Monit., 19(6):609 (1997)
9. Gurley. Drug Metab Dispos., 35(2) (2007)
10. Gurley. Drug Metab Dispos., 34(1): 69 (2006)
11. Rengelhausen. Br J Clin Pharmacol., 56:32 (2003)
12. Tsutsumi. J Clin Pharmacol., 42:1159 (2002)
13. Hager. Eng J Med., 300(22):1238 (1979)
14. Ochs. Amer Heart J., 96(4):507 (1978)
15. Erjrfalt. Mol Pharm., 12(11):4166 (2015)
16. Westphal. Clin Pharmacol Ther., 68(1):6 (2000)
17. Tayrouz. Clin Pharmacol Ther., 73(5):397 (2003)
18. Johnson. Clin Pharmacol Ther., 23(3):315 (1978)
19. Greenblatt. Clin Pharmacol Ther., 16(3):448 (1974)
20. Jounela. Eur J Clin Pharmacol., 8 :365 (1975)
21. Guest. Drug Metab Dispos., 39(2) :170 (2011)
22. Hinderling. J Pharm Sci., 73(8): 1042-1053 (1984)
23. Florence. J Pharm Pharmacol., 28(8): 637-642 (1976)
24. Lu. Pharm Res., 10(9):1308-1314 (1993)
25. Varma. J Pharm Sci., 94(8): 1694-1704 (2005)
26. FDA Label: Lanoxin (2016)
27. Kishimoto et al. DMD., 42(2): 257-263(2014)
28. Isoherranen et al. DMD., 32(10) : 1121-1131 (2004)
29. Eberl et al. Clin Pharmacokinet., 46(12): 1039-1049 (2007)
30. Asaumi et al. CPT :PSP., 7(3) : 186-196 (2018)
31. Kajosaari et al. Clin Pharmacol Toxicol., 97(4): 249-256 (2005)
32. Yoshikado et al. Clin Pharmacol Ther., 100(5): 513-523. (2016)
33. Morse et al. CPT:PSP.m 8(9) : 664-675 (2019)
34. Asaumi et al. CPT :PSP.,11(7) : 919-933 (2022)
35. Lutz et al. CPT., 104(6) : 1182- 1190 (2018)

SimulationsPlus
SCIENCE + SOFTWARE = SUCCESS